Hydrothermal synthesis of solvents assisted SnO_2 nanoparticles and their optical properties

J. GAJENDIRAN*, V. RAJENDRAN
Department of Physics, Presidency College, Chennai-600 005, Tamilnadu, India

A comparative study of size, morphology, surface area and optical properties of tin oxide (SnO_2) nanoparticles has been reported in this article. SnO_2 nanoparticles have been successfully synthesized by using different solvents such as water, water-butanol and water-ethylene glycol via hydrothermal method. X-ray powder diffraction (XRD), Scanning electron microscopy (SEM), Transmission electron microscopy (TEM), Energy dispersive X-ray spectra (EDX), UV–vis absorption and Photoluminescence (PL) spectra were used to characterize the calcined SnO_2 samples. XRD analysis revealed that all relevant Bragg reflection for tetragonal rutile structure of SnO_2 nanoparticles. The non-uniform, uniform, and well dispersed spherical nanoparticles like morphologies of the calcined water, water-butanol and water-ethylene glycol mediated SnO_2 samples in the SEM and TEM images. The band gap energies were calculated to be 3.73, 3.78 and 3.81eV from the UV-vis absorbance spectra. PL emission spectra show that the SnO_2 nanoparticles generate a visible light emission that acts as a luminescent centre.

(Received June 1, 2011; accepted September 18, 2013)

Keywords: Semiconductor, SnO_2, solvents, hydrothermal method, Optical properties

1. Introduction

In recent years, there has been a tremendous increase in research activity in the field of nanosized materials. This is because interesting variations in the properties of materials in nanosized configuration as compared to their bulk counterparts, and hence their novel application potential. The size, shape and crystal structure of nanosized materials are important parameters that have control their chemical, optical and electrical properties. Metal oxide semiconductors are extensively used in the production of commercial gas sensors. SnO_2 sensors have been dominated among these due to their high sensitivity, quick response, resistance to corrosion, etc. [1-3].Tin oxide is an n type semiconductor with excellent optical and electrical properties, partly due to its wide band gap (E_g = 3.6 eV at 300K). Nanosized SnO_2 has been extensively investigated in various areas, such as transparent conductive electrodes and transistors [4-7], Li-ion batteries [8,9], dye-sensitize solar cells [10], and chemical gas sensors [11-12]. Till now many methods have been developed to synthesize SnO_2 nanocrystallites, including sol- gel [13], chemical vapor deposition [14], annealing precursors powders [15,16], thermal evaporation [17] and microwave heating [18]. Among the other methods, the hydrothermal approach is a better alternative with the advantages of high purity, controlled stoichiometric, microstructure, morphology, homogenity, high crystallinity, narrow particle size distribution and low environmental pollution. The hydrothermal processing is alternative to calcinations for the crystallization of SnO_2 under mild temperatures. Poly (ethylene glycol) (abbreviated as PEG), is known to be able to provide an inexpensive, thermally stable and non-toxic reaction medium [19].

Starting from tin chlorides ($SnCl_4$ or $SnCl_2$) is generally preferred because they are easy to performs and the cost is very low, but the chlorine ions are very difficult to remove and the residual chlorine ions often affect the surface and electrical properties, introducing a random n-type doping in the material [20], modifying the sensitivity of sensors [21], causing agglomeration among particles [22] and leading to higher sintering temperatures [23]. In the chemical methods reported in the literature the most common precursor used was $SnCl_4{\cdot}5H_2O$ with the oxidation state IV of tin in solution leading to the formation of SnO_2 nanocrystals [24-27].

The main purpose of the present research is to study the influence of water, water-butanol and water-ethylene glycol solvents on the size, morphology, surface area and optical properties of the SnO_2 nanoparticles were investigated.

2. Experimental

All chemical reagents were commercial with AR purity, and used directly without purification.$SnCl_4.5H_2O$ (4.532 g) was dissolved in 10 ml of water. Then 3g of sodium hydroxide pellet was dissolved in 10 ml of distilled water. These solutions were added drop-wisely to the well-stirred solution until forming a transparent solution. A total of 25 ml of PEG-400 was put into the above solution with stirring for about 10 min. Then, the above solution with was loaded into a 75 ml Teflon-lined stainless autoclave. The autoclave was sealed and maintained at 150 ºC for 4 h, followed by cooling it to room temperature. The white precipitate was obtained and was washed several times with distilled water and absolute ethanol. Then dried in vacuum at 60 ºC for 4 h and then

obtained ash colored samples was calcined at 450 ºC for 2 h. Finally, white colored SnO_2 powders were obtained. The same procedure was followed for the white, pale yellow colored SnO_2 powders using solvent such as water-butanol and water-ethylene glycol.

A similar mechanisms was reported by Hongling Zhu et al, in tin oxide nanoparticles via hydrothermal method [28]. As we can expect like this formation mechanism might applicable to our current synthetic procedure water instead of using water-butanol and water-ethylene glycol.

The obtained samples were characterized by X-ray powder diffraction (XRD). XRD pattern was collected on a schimadzu model; XRD 6000 with CuKα radiation (λ= 1.547 Å), at scanning rate of 0.04 s^{-1} was applied to record the pattern in the range 20–70º. The specific surface area of SnO_2 samples can be roughly calculated by using $S= 6* 10^4 /\rho*D$ formula. Where ρ = density, D = Average grain size. Scanning electron microscope (SEM) analysis was carried out for the sample on a JEOL- JSM - 67001 SEM. Transmission electron microscopy (TEM) was carried out on CM-20 TEM using accelerating voltage 100 kV. Energy dispersive X-ray spectrum analysis (EDS) were carried out for the sample on a Philips model CM-20 TEM. UV-Vis absorption spectra of the samples were recorded at room temperature by using Varian cary5E spectrophotometer. The photoluminescence (PL) spectra were recorded by Fluoromax-4 spectrofluorometer with a Xe lamp excitation light source.

3. Results and discussion

Fig 1(a-c) (water, water-butanol and water-ethylene glycol) shows the XRD patterns of the SnO_2 nanoparticles calcined at 450 ºC. All the samples are crystalline and the diffraction peaks can be indexed as the tetragonal rutile structure, which is consistent with the reported data (JCPDS file no.77-0450). No other phase can be detected. The diffraction peaks are markedly broad, which indicates that the crystallite sizes of samples are small. The average crystallite size is about 6 nm at water-ethylene glycol medium, which is the smallest to the other solvents such as water, water-butanol. Using Debye-scherrer's equation ($D = 0.89\lambda/\beta\cos\theta$), the average crystallite sizes of SnO_2 nanoparticles could be determined. The average crystallite size, particle size, surface morphology, surface area and band gap of calcined SnO_2 nanoparticles are tabulated in Table1.

Assuming the particles to be a sphericity, the specific surface area of SnO_2 samples could be roughly calculated to be 95.37, 107.29 and 143.06 m^2g^{-1} by using $S = 6* 10^4 /\rho*D$ formula.

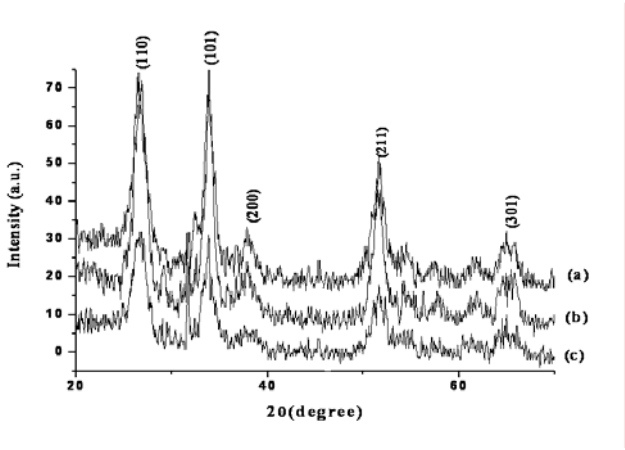

Fig. 1 XRD patterns of the SnO_2 nanoparticles calcined at 450ºC solvent mediated (a) water, (b) water-butanol, and (c)water-ethylene glycol.

Table 1 Different properties of as-synthesized SnO_2 nanoparticles.

SnO_2samples	Crystallite size (nm)	Particle size (nm)	morphology	Surface area (m^2/g)	Band gap (eV)
Water	9	~ 9-9.5	Non-uniform spherical	95.37	3.73
Water-butanol	7	~ 7-8	Uniform spherical	107.29	3.78
Water-ethylene glycol	6	~ 6-6.5	Uniform spherical	143.06	3.81

The surface morphology of the samples obtained using water; water-butanol and water-ethylene glycol as examined by SEM is shown in Fig. 2 (a-c). Non-uniform spherical-like morphologies were observed for the figure 2a (water).

The uniform spherical morphologies were observed for the Fig. 2b (water-butanol).The uniform spherical like morphology was also observed for the Fig. 2c (water-ethylene glycol).

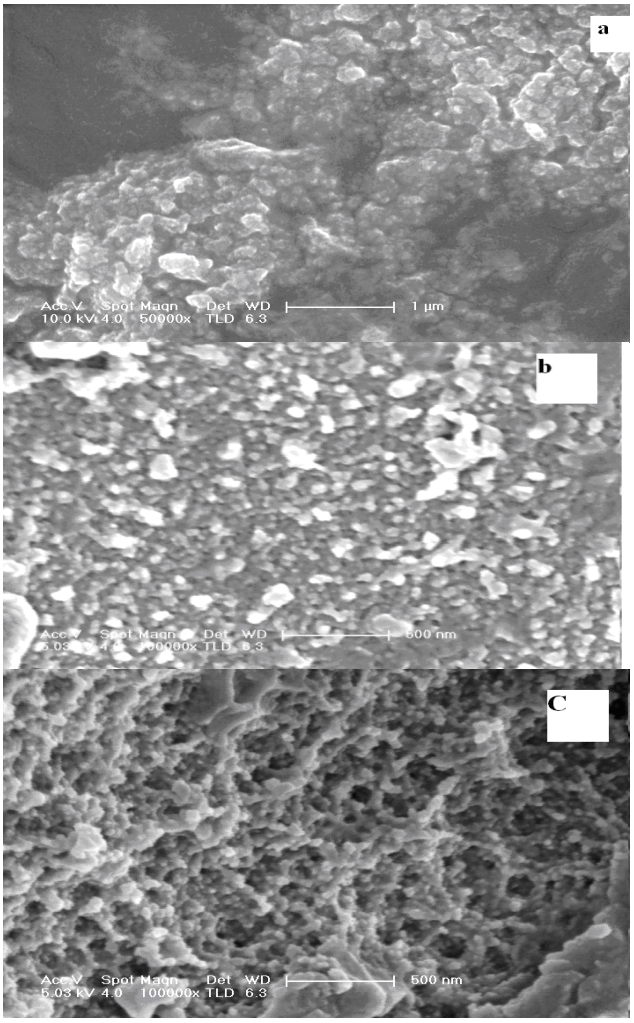

Fig. 2. SEM image s of SnO_2 nanoparticles solvent mediated (a) water (b) water-butanol and (c) water-ethylene glycol.

Fig. 3 shows TEM image of the SnO_2 nanoparticles calcined at 450 ºC. The non-uniform spherical-like morphology of aggregated water mediated SnO_2 nanoparticles with particle size range from ~9-9.5nm. However, the uniform spherical-like morphology with particle size ranges from ~ 7-8nm, which is weakly, aggregated. The well dispersed fine spherical like morphologies were observed for the sample with average particle size ~ 6-6.5 nm, which is consistent with the SEM (Fig. 2c) and XRD analysis (Fig..1c). The different particle size reveals the key role of individual solvent in controlling the abrupt nucleation and crystal orientation. Smaller nanoparticles were observed in water-ethylene glycol mediated SnO_2 sample. Because water-ethylene glycol might form a protective layer around the particle surface via the interaction of its OH group with the surface of precipitate, preventing the particle agglomeration. The size of primary nanoparticles can be determined from dark-field imaging by this study. Use of dark-field image for determining the particle is preferred over X-ray line broadening [29].

The selected area electron diffraction (SAED) pattern of SnO_2 nanoparticles prepared from the various solvents as shown in the inset of Fig. 3(a-c).All the ring patterns exhibit the lattice planes such as (110), (101), (200), (211), (301) have the single crystalline nature of the tetragonal rutile structure of SnO_2 nanoparticles, which is good agreement with the XRD patterns.

Fig. 4 shows that the EDX pattern of the ethylene glycol assisted SnO_2 nanoparticles at 450ºC. The sample was composed weighted percentage of Sn -85.50 % and O-14.40 % which clearly indicates that the synthesized sample is tin oxide (SnO_2) nanoparticles.

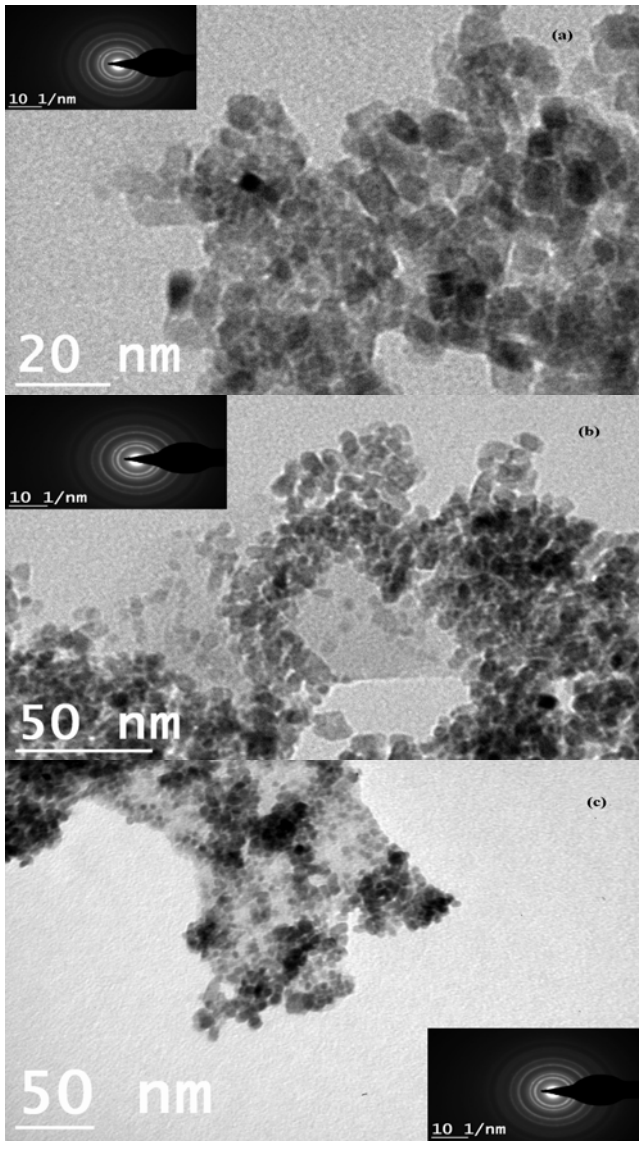

Fig. 3. TEM images of SnO_2 nanoparticles solvent mediated (a) water (b) water-butanol and (c) water-ethylene glycol

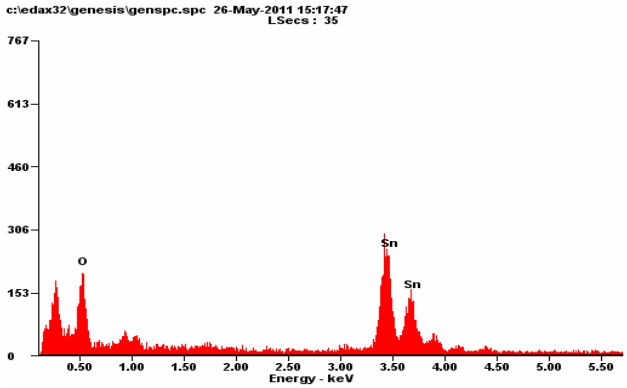

Fig. 4. EDX spectrum of ethylene glycol mediated SnO_2 nanoparticles.

UV–vis absorption spectrum which has been extensively studied is one of the most important methods to reveal the energy structures and optical properties of semiconductor nanostructures. Fig. 5 represents the UV absorption spectra of SnO_2 nanoparticles, and absorbance edges were observed at 332, 328, and 325 nm for different solvent mediated like water, water-butanol and water-ethylene glycol respectively (Fig. 5(a-c)). In all the cases, the blue shifts were observed. Considering the blue shift of the of the absorption onsets of the presents samples can be assigned to the direct transition of electron in the SnO_2 nanoparticles. The corresponding band gap energies can be calculated to be 3.73, 3.78 and 3.81 eV and are larger than the bulk SnO_2 (E_g=3.6 eV) [30].

The PL emission spectra of SnO_2 samples such as water, water-butanol and water-ethylene glycol are shown in Fig. 6(a-c). The water mediated SnO_2 sample presents are not an intense PL band in both UV and visible regions (Fig. 6a). However, the water-butanol and water-ethylene glycol mediated SnO_2 samples shows an intense strong abide PL band centered at ~ 400 nm together with a shoulder peak at 413,420,445,450,463,467,473 and 482 nm in both cases (Fig. 6b and 6c).

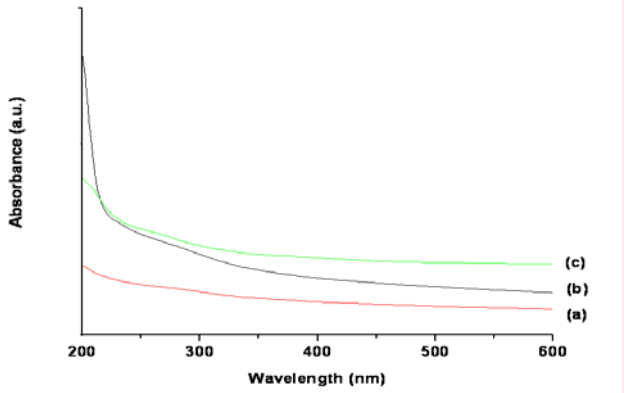

Fig. 5. UV-Vis absorption spectra of the SnO_2 nanoparticles solvent mediated (a)water (b) water-butanol, and (c) water-ethylene glycol.

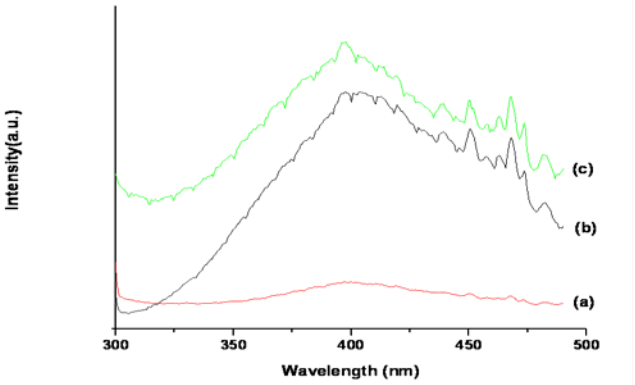

Fig. 6 Emission spectra of the SnO_2 nanoparticles solvent mediated (a) water, (b) water-butanol, and (c) water-ethylene glycol.

The UV emission in SnO_2 samples is attributed to electron transition mediated by defect levels in the bandgap, such as oxygen vacancies [31-34]. The origin of the emission band at 445 nm is not clear. Gu et al.[32] put forward that this band might originate from the luminescent centres formed by such tin interstitials or dangling in SnO_2 nanoparticles, but the detail was not discussed. Cheng et al. [35] proposed that this band may be related to crystal defects or defect levels associated with oxygen vacancies, or tin interstitials. Das et al. [36] pointed out that the visible emission band around 400–500 nm for SnO_2 nanoparticles can be assumed to be due to the formation of luminescent centre. The well known stronger and broader emission situted (except Fig. 6a Low intensity UV and visible emission signal) in the yellow-green part of the visible spectra is much lower, which suggests that the as-obtained SnO_2 samples are high pure and crystalline with a rather low concentration of oxygen vacencies.

4. Conclusions

Hydrothermal synthesis of SnO_2 nanoparticles have been successfully synthesized by using different solvents such as water, water-butanol and water-ethylene glycol. The XRD pattern revealed that the obtained products exhibit tetragonal rutile structure of SnO_2.The particle sizes of the SnO_2 nanoparticles calcined at 450ºC in water, water-butanol and water-ethylene glycol were 6, 7 and 9 nm, respectively which is confirmed by XRD results. On the other hand, the morphologies of the SnO_2 nanoparticles are dependent on the solvent. Therefore, solvent play an important role in the preparation of metal oxide nanoparticles. The band gap energies are calculated to be 3.73, 3.78 and 3.81eV from the UV-Vis absorbance spectra. PL emission spectra show that the SnO_2 nanoparticles generate a visible light emission that acts as a luminescent centre. Moreover, the small size SnO_2 nanoparticles would be promised in the applications of sensor, solar cell and optical electronic devises.

Acknowledgment

The authors are grateful to the Tamilnadu State council for Science and Technology, for extending financial assistance to carry out this work.

Reference

[1] S.R.Morrison, Sens. Actuators **2**, 329 (1982).
[2] P.T.Moseley , Meas.Sci.Technol, **8**, 223 (1997).
[3] J.Watson , K.Ihokura , G.S.V.Coles , Meas. Sci. Technol, **4**, 711 (1993).
[4] S.Papargyri, D.N.Tsipas, D.A.Papargyris,A.I.Botis, Athanasios D.Papargyris, Solid state Phenomena, **106**, 57 (2005).
[5] S.Mathur, S.Barth , H.Shen , J.C.Pyun, U.Werner, Small, **1**, 713 (2005).
[6] Z.Q.Liu, D.H.Zhang, S.Han, C.Li, T.Tang, W.Jin, X.L.Liu,B.Lei, C.W.Zhou , Adv.Mater, **15**, 1754 (2003).
[7] E.N.Dattoli , Q.Wan, W.Guo, Y.Chen ,X.Q.Pan, W. Lu , Nano Lett, **7**, 2463 (2007).
[8] S. H. Ng, D. L. Dos Santos, S. Y. Chew, D. Wexler, J. Wang, S. X. Dou, H. K. Liu, Electrochem.Commun, **9**, 915 (2007).
[9] M. S. Park, G. X. Wang, Y. M. Kang, D. Wexler, S. X. Dou, H. K. Liu, Angew. Chem. Int.Ed, **46**, 750 (2007).
[10] S. Ferrere, A. Zaban, B. A. Gregg, J. Phys. Chem., B **101**, 4490 (1997).
[11] J. Xu, D. Wang, L. Qin, W. Yu, Q. Pan, Sensors Actuators B:Chemical, **137**, 490 (2009).
[12] Q. Dong, H. L. Su, J. Q. Xu, D. Zhang, Sens. Actuators, B **123**, 420 (2007).
[13] J. Zhang, L. Gao, chemistry lett, **32**, 458 (2003).
[14] Y. Liu, J. Dong, M. Liu, Adv. Mater,**16**, 353 (2004).
[15] C. Nayral, E. Viala, P. Fau , F.Senocq, J. C. Jumas, A. Maisonnat, B. Chaudret, Chem. Eur. J, **6**, 4082 (2000).
[16] Y. Liu, C. Zheng, W. Wang, C. Yin, G. Wang, Adv. Mater, **13**, 1883 (2001).
[17] Z. R. Dai, Z. W. Pan, Z. L. Wang, Adv. Funct. Mater, **13**, 9 (2003).
[18] J. J. Zhu, J. M. Zhu, X. H. Liao, J. L. Fang, M. G. Zhou, H. Y. Chen, Mater. Lett, **53**, 12 (2002).
[19] V. V. Namboodiri, R. S. Varma, Green Chem, **3**, 146 (2001).
[20] J. S. Pena, T. Brousse, L. Sanchez, J. Morales, D. M. Schleich, J. Power Sources, **97-98**, 232 (2001).
[21] N. Sergent, P. Gelin, L. Perier-Camby,H. Praliaud, Thomas, Sensors Actuators, **B84**, 176 (2002).
[22] A. Roosen, H. Hausner, Adv. Ceram. Mater, **3**, 131 (1998).
[23] O. Vasylkiv, Y. Sakka , J. Am. Ceram. Soc, **84**, 2489 (2001).
[24] F. Du ,Z. Guo, G. Li , Mater.Lett **59**, 2563 (2005).
[25] F. Paraguay-Delgado, W. Antunez-Flores, M. Miki-Yoshida, A. Aguilar-Elguezabal, P. Santiago, J. R. Diaz, J. A. Ascencio , Nanotechnology, **16**(6), 688 (2005).
[26] Z. W. Chen, J. K. L. Lai, C. H. Shek, J. Non-Cryst.Solids , **351**, 3619 (2005).
[27] N. Shirahata, A. Hozumi, S. Asakura, A. Fuwa, Y. Sakka, J. Vac. Sci.Technol, A **23**, 731 (2005).
[28] Z. Hongllang, Y. Deren, Y. Gulxla, Z. Hul, Y. Kulhong, Nanotechnology, **17**, 2386 (2006).
[29] G. M. Chow, K. E.Gonsalves ,(Institute of physics publishing) , Bristol and Philadelphia **6**, 305 (1996).
[30] A Aoki, H Sarakura, Jpn. J.Appl.Phys, **9**, 582 (1970).
[31] F. Gu, S. F. Wang, M. K. Lu, X. F. Cheng, S. F. Liu, G. J. Zhou, D. Xu, D. R. Yuan, J. Cryst. Growth **262**, 182 (2004).
[32] F. Gu, S. F. Wang, C. F. Song, M. K. Lu, Y. X. Qi, G. J. Zhou, D. Xu, D. R. Yuan, Chem. Phys. Lett, **372**, 451 (2003).
[33] N. Dharmaraj, C. H. Kim, K. W. Kim, H. Y. Kim, E. K. Suh, Spectrochimica.Acta .Part *A* Molecular and Biomolecular Spectroscopy, **64**, 136 (2006).
[34] J. X. Zhou, M. S. Zhang, J. M. Hong, Z. Yin, Solid State Commun, **138**, 242 (2006).
[35] B. Cheng, J. M. Russell, W. Shi, L. Zhang, E. T. Samulshi, J. Am. Chem.Soc, **126**, 5972 (2004).
[36] S. Das , S. Kar, S. Chaudhuriy, J.Appl. Phys, **99**, 114303 (2006).

*Corresponding author: gaja_1986msc@yahoo.co.in